

# Resonant tunneling through a double GaAs/AlAs superlattice barrier, single quantum well heterostructure

M. A. Reed, J. W. Lee, and H-L. Tsai

Central Research Laboratories, Texas Instruments Incorporated, Dallas, Texas 76265

(Received 18 April 1986; accepted for publication 20 May 1986)

Resonant tunneling has been demonstrated through a double barrier, single quantum well heterostructure in which the barriers have been replaced by thin, short period binary superlattices. The superlattice structure does not exhibit the asymmetry around zero bias in the electrical characteristics normally observed in the conventional  $\text{Al}_x\text{Ga}_{1-x}\text{As}$  barrier structures, suggestive of reduced roughness at the inverted interface by superlattice smoothing. The structure exhibits an anomalously low barrier height and a peak to valley tunnel current ratio of 1.8:1 at 300 K.

The phenomenon of resonant tunneling in double barrier heterostructures, first investigated in the seminal work of Chang, Esaki, and Tsu,<sup>1</sup> has recently undergone a renaissance<sup>2-4</sup> due to recent improvements in epitaxial growth techniques. The dc and high-frequency transport in these structures has been the subject of intense investigation following the remarkable submillimeter wave experiments of Sollner *et al.*,<sup>2</sup> which has been interpreted as coherent resonant tunneling through the heterostructure. This renewed interest has led to the observation of large room-temperature peak to valley tunnel current ratios,<sup>4</sup> resonant tunneling of holes,<sup>5</sup> the observation of multiple negative differential resistance (NDR) peaks due to resonant tunneling,<sup>6</sup> and the observation of sequential resonant tunneling through a multi-quantum well (MQW) superlattice.<sup>7</sup>

The initial investigations of this structure, typically in the GaAs/ $\text{Al}_x\text{Ga}_{1-x}\text{As}$  system, have utilized "square" (i.e., constant Al mole fraction) barriers to confine the central quantum well. A number of intriguing physical phenomena can be examined by tailoring the barrier(s) in real space, such as equally spaced resonant peaks arising from a parabolic quantum well.<sup>8</sup> However, the variety of tunneling structures that can be investigated is limited by the practical constraints on the  $\text{Al}_x\text{Ga}_{1-x}\text{As}$  barrier (or well) growth and the rate the Al mole fraction can be changed over the region of interest, typically  $\sim 100 \text{ \AA}$ . A possible solution to the Al mole fraction gradient constraint is the emulation of the desired  $\text{Al}_x\text{Ga}_{1-x}\text{As}$  alloy barrier structure with a GaAs/ $\text{Al}_x\text{Ga}_{1-x}\text{As}$  superlattice of fixed (even 100%) Al mole fraction.<sup>9-11</sup> In this letter we report the first study of resonant tunneling through a double barrier, single quantum well heterostructure in which the barriers have been replaced by very thin, short period superlattices and that resonant tunneling transport through a compositional modulated barrier is possible.

The samples used in this study were grown by molecular beam epitaxy in a Riber MBE-2300 on a 2-in. (100)  $n^+$  Si-doped Sumitomo GaAs substrate utilizing a directly heated rotating substrate holder. Following a highly doped ( $n$  type, Si @  $1 \times 10^{18} \text{ cm}^{-3}$ ) buffer layer, the active resonant tunneling structure region was then grown. For comparison, a con-

ventional  $\text{Al}_x\text{Ga}_{1-x}\text{As}$  alloy barrier structure of similar barrier and quantum well dimension was fabricated, as well as one with a larger quantum well size. The conventional  $\text{Al}_x\text{Ga}_{1-x}\text{As}$  barrier sample consisted of an undoped  $\text{Al}_x\text{Ga}_{1-x}\text{As}$  barrier (50  $\text{ \AA}$ ,  $x = 0.35$ ), followed by an undoped GaAs quantum well (50 and 100  $\text{ \AA}$ ), similar barrier, and a top contact  $\sim 0.5 \mu\text{m}$  thick. For the binary superlattice barrier structure, each barrier consists of three 7  $\text{ \AA}$  layers of AlAs separated by two 7  $\text{ \AA}$  layers of GaAs. The GaAs quantum well in this sample is 45  $\text{ \AA}$  and the remainder of the structure is identical to the  $\text{Al}_x\text{Ga}_{1-x}\text{As}$  barrier samples. A cross-sectional transmission electron micrograph of the superlattice barrier structure is shown in Fig. 1. Devices were fabricated by defining mesas on the surface with conventional photolithography techniques, bonded for mechanical stability, and inserted into a variable-temperature helium-flow Janis cryostat or into a stabilized oven for variable temperature measurements.

Figure 2(a) shows the room-temperature static current-voltage ( $I$ - $V$ ) characteristics of a typical conventional alloy barrier, 50- $\text{ \AA}$ -wide quantum well, resonant tunneling structure. This structure exhibits a room-temperature peak to val-

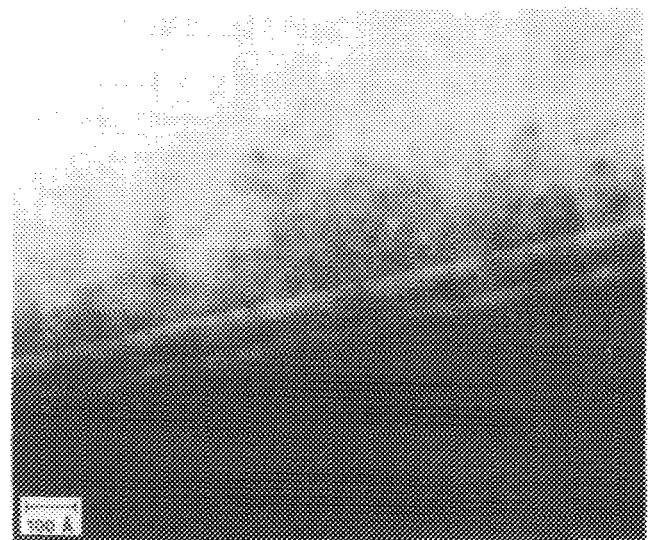


FIG. 1. Cross-sectional transmission electron micrograph of the superlattice barrier resonant tunneling structure. The width of the GaAs quantum well is 45  $\text{ \AA}$  and the widths of the two GaAs and three AlAs superlattice barrier components are 7  $\text{ \AA}$ .

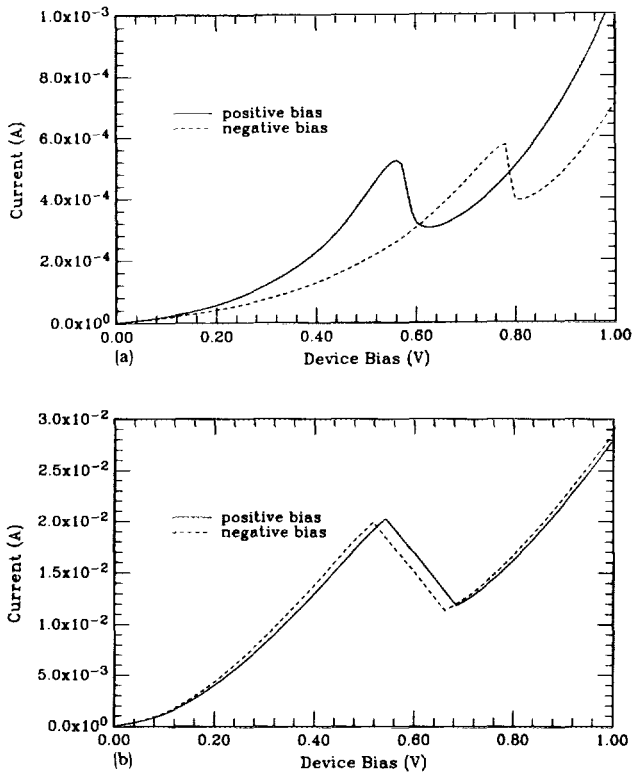


FIG. 2. (a) Room-temperature static  $I$ - $V$  characteristics of a typical conventional 50 Å alloy barrier, 50 Å wide quantum well, resonant tunneling structure. Device mesa area = 25  $\mu\text{m}^2$ . Positive and negative bias are shown. (b) Room temperature static  $I$ - $V$  characteristics for the superlattice barrier structure. Device mesa area = 25  $\mu\text{m}^2$ . The symmetry for positive and negative bias is excellent.

ley tunnel current ratio of 1.75:1 which increases typically to 7:1 at low temperatures ( $\leq 100$  K). We have plotted the negative bias data reflected into the first quadrant to emphasize the observed asymmetry in the current-voltage characteristics of these structures. This asymmetry has been ascribed to the inferior inverted interface morphology of the quantum well and contact region.<sup>4</sup> This is consistent with our observations; our convention of positive bias means electron injection from the backside superior GaAs contact. A higher resonant bias for the inverted configuration would be expected from an extended inverted region. The room temperature  $I$ - $V$  characteristics for the superlattice barrier structure, designed to have the same resonant bias voltage, is shown in Fig. 2(b). The symmetry for positive and negative bias is excellent. This observation suggests that the inverted interface is indeed responsible for the observed asymmetry in the alloy barrier structure and that the superlattice barrier improves the interface by lessening trapping of undesired impurities and/or prevents surface roughening. This improvement has been observed previously in photoluminescence experiments.<sup>10</sup> The superlattice barrier structure exhibits a 1.8:1 peak to valley ratio at room temperature and exhibits NDR up to 100 °C.

The observed resonant bias positions can be compared to the theoretical predictions of a transfer matrix model<sup>12</sup> if the parasitic resistances in the structure are independently known. Since this is unknown for the structures, we employ

the technique<sup>13</sup> of low bias thermal activation of carriers over the effective barrier to determine the position of the quantum well bound state relative to the Fermi level of the contact. In this case the effective thermal barrier presented to the electrons, at low bias, is not the full barrier but the  $\Gamma$  point of the quantum well bound state. This is demonstrated in Fig. 3(a) for the alloy barrier structure with a 50 Å quantum well, which yields an activation energy of 70 meV. Similar measurements on an alloy barrier structure with a quantum well width of  $\sim 100$  Å gave an activation energy of 15 meV, demonstrating that the activation energy decreases with increasing well size as expected. It should be noted that the ground state only is observed due to the large energetic separation of the excited state.

The activation energy gives the quantum well energy relative to the conduction-band edge when corrected for the assumed degeneracy in the contact due to the high doping ( $N_D \approx 1 \times 10^{18} \text{ cm}^{-3}$ , which gives  $E_F \approx 55$  meV). The derived quantum well state is 120 meV which is in excellent agreement with the values of 116 meV predicted from an envelope function approximation<sup>14</sup> using a 60% conduction-band offset. This technique was used to derive the position of the center quantum well state for the superlattice barrier structure and is shown in Fig. 3(b) for two devices of different mesa dimension. The thermal activation measurement for both gives a quantum well state of 121 meV, the same as the 50 Å alloy barrier structure which was expected from the identical resonant bias positions (without the inverted bias asymmetry complication) of Fig. 2.

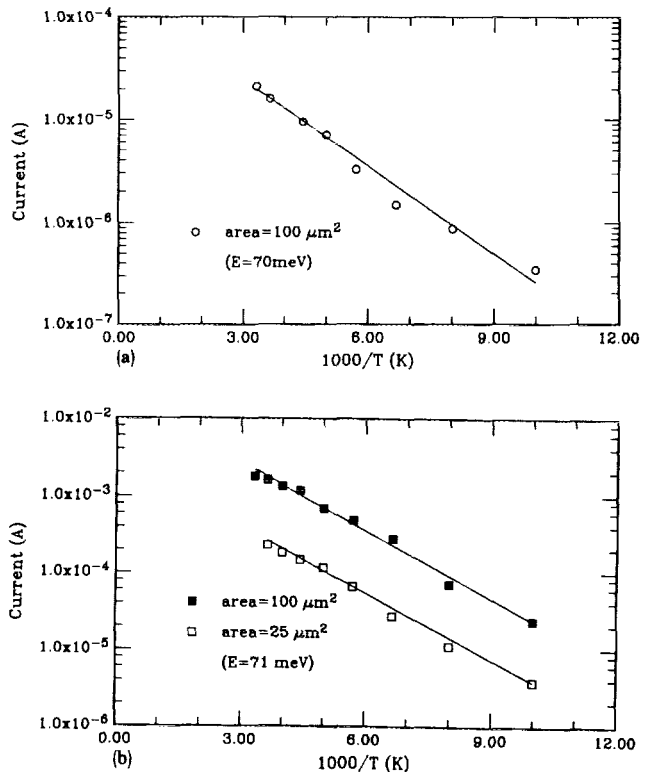


FIG. 3. (a) Low bias thermally activated current for the 50 Å quantum well alloy barrier structure. The thermal activation measurement gives  $E = 70$  meV. (b) Low bias thermally activated current for the superlattice barrier structure, showing identical activation energies independent of current density. The current does not exactly scale with top mesa dimension due to mesa undercut. The thermal activation measurement gives  $E = 71$  meV.

There are two independent approaches to determine the effective barrier height  $\Delta E_c^*$  of the superlattice barrier once the quantum well energy is known. Firstly, we can use the energy of the quantum well state (determined above) to derive the effective barrier height  $\Delta E_c^*$  assuming that the envelope function approximation for thick barriers is valid. Using a 45 Å quantum well, we obtain an effective barrier height  $\Delta E_c^* = 290$  meV, or an equivalent alloy composition of 0.296.

Secondly, we can compare the transmitted resonant current densities of the conventional alloy barrier structure and the superlattice barrier structure. Considering single particle transmission coefficients, it can be shown that the effective barrier height  $\Delta E_c^*$  can be expressed as

$$\Delta E_c^* = E_{QW,0}^{SL} + \frac{\hbar^2}{8m^*d_{SL}^2} \times \left( \ln \frac{J_{SL}}{J_A} + \frac{2d_A}{\hbar} [2m^*(\Delta E_c^A - E_{QW,0}^A)]^{1/2} \right),$$

where  $d_{SL}$  is the width of the superlattice barrier,  $d_A$  is the width of the alloy barrier,  $J_A$  and  $J_{SL}$  are the measured current densities for the alloy barrier and superlattice barrier, respectively,  $\Delta E_c^A$  is the conduction-band offset for the alloy barrier case, and the  $E_{QW,0}^A$  are the ground state energies of the quantum wells. Using a 60% conduction-band offset and a 35 Å superlattice barrier width, we get  $\Delta E_c^* = 240$  meV, slightly lower than the barrier computed above. A monolayer fluctuation at the interfaces of the barrier gives  $\Delta E_c^* = 275$  meV, in good agreement with the envelope function prediction. The evanescent tail contribution, clearly important here, lowers the thick barrier envelope function prediction for the quantum well state.

The superlattice barrier height is much lower than would be expected from an averaged alloy composition of 0.60, which gives a barrier height of 587 meV. Photoluminescence experiments on thick superlattice barrier confined isolated quantum wells<sup>10</sup> also found disagreement with an averaged alloy composition model, although an equivalent alloy composition higher than the average alloy composition was found. An envelope function approximation to a superlattice of infinite extent to determine the effective barrier height as the first conduction minizone edge gives an even greater discrepancy. Thus the superlattice barrier allows appreciable wave function penetration while maintaining a high-energy quantum well state, as has been previously suggested.<sup>10</sup> The observation of an anomalously low barrier

height to transport is indicative of the enhanced evanescent tail.

The ability to emulate barriers with superlattices permits a number of intriguing suggested investigations for tunneling structures, such as equally spaced resonances from a parabolic well, an increase in transmission coefficient from a structure symmetric at resonant bias, band-gap engineered contacts, an increase in sequential multiquantum well resonant current, and the investigation of the influence of barrier symmetry on resonant bias and transmission. The flexibility of design and enhanced evanescent tail are also important to MQW lasers and high-frequency resonant tunneling devices.

In summary, we have reported the first study of a double short period binary superlattice barrier, single quantum well heterostructure. This is the first demonstration that quantum well states can be confined by very thin, short period superlattices. The superlattice structure does not exhibit the asymmetry around zero bias in the electrical characteristics normally observed in the conventional  $Al_xGa_{1-x}As$  barrier structures, and exhibits an anomalously low barrier height demonstrating an enhanced evanescent tail in the superlattice barrier.

We are thankful to R. T. Bate, W. R. Frensley, and C. H. Hoel for discussions and R. Aldert, R. Thomason, and J. Williams for technical assistance. This work was supported in part by the Office of Naval Research and the U.S. Army Research Office.

<sup>1</sup>L. L. Chang, L. Esaki, and R. Tsu, *Appl. Phys. Lett.* **24**, 593 (1974).

<sup>2</sup>T. C. L. G. Sollner, W. D. Goodhue, P. E. Tannenwald, C. D. Parker, and D. D. Peck, *Appl. Phys. Lett.* **43**, 588 (1983).

<sup>3</sup>A. R. Bonnefoi, R. T. Collins, T. C. McGill, R. D. Burnham, and F. A. Ponce, *Appl. Phys. Lett.* **46**, 285 (1985).

<sup>4</sup>T. J. Shewchuk, P. C. Chapin, P. D. Coleman, W. Kopp, R. Fisher, and H. Morkoç, *Appl. Phys. Lett.* **46**, 508 (1985).

<sup>5</sup>E. E. Mendez, W. I. Wang, B. Ricco, and L. Esaki, *Appl. Phys. Lett.* **47**, 415 (1985).

<sup>6</sup>M. A. Reed, *Superlattices and Microstructures* (in press).

<sup>7</sup>F. Capasso, K. Mohammed, and A. Y. Cho, *Appl. Phys. Lett.* **48**, 478 (1986).

<sup>8</sup>F. Capasso and R. A. Kiehl, *J. Appl. Phys.* **58**, 1366 (1985).

<sup>9</sup>W. D. Laidig, P. J. Caldwell, K. Kim, and J. W. Lee, *Electron. Device Lett.* **4**, 212 (1983).

<sup>10</sup>H. Sakaki, M. Tsuchiya, and J. Yoshino, *Appl. Phys. Lett.* **47**, 295 (1985).

<sup>11</sup>K. Fujiwara, J. L. de Miguel, and K. Ploog, *Jpn. J. Appl. Phys. Part 2*, **24**, L405 (1985).

<sup>12</sup>B. Ricco and M. Ya. Azbel, *Phys. Rev. B* **29**, 1970 (1984).

<sup>13</sup>A. C. Gossard, W. Brown, C. L. Allyn, and W. Wiegmann, *J. Vac. Sci. Technol.* **20**, 694 (1982).

<sup>14</sup>G. Bastard, *Phys. Rev. B* **24**, 5693 (1981).